Location of Optical Transitions in $\vec{k}$ space from Angular Photoemission Measurements on W†

R. R. Turtle and T. A. Callcott
Department of Physics, University of Tennessee, Knoxville, Tennessee
(Received 4 September 1974)

The energy and emission angle of electrons photoemitted from the (110) and (111) surfaces of W have been measured for photon energies between 7.7 and 10.7 eV. For prominent transitions, the component of internal $\vec{k}$ vector tangential to the surface was obtained from angular measurements on each of the two surfaces. The two components of $\vec{k}$ were used to determine the internal $\vec{k}$ vector of prominent transitions occurring in the plane defined by the ⟨110⟩ and ⟨111⟩ axes.

It is well known that the angular distribution of photoemitted electrons contains information about the crystal momentum (or wave vector $\vec{k}$) of the states involved in the photoexcitation process. However, previous papers on angular photoemission have not demonstrated the feasibility of determining the wave vectors of states participating in direct optical transitions by photoemission measurements alone. Feurbacher and Fitton measured emission normal to three single-crystal faces of W in order to study only those direct transitions occurring along principal crystalline axes, but, as will be shown, missed observing a strong group of transitions causing emission in directions between the ⟨110⟩ and ⟨111⟩ axes.[1] Other workers[2,3] have published studies of angular photoemission. They have derived values of the wave vectors of states participating in the emission process, but have eliminated the uncertainty in the normal component of $\vec{k}$ inside the crystal by means other than photoemission measurements. In this paper we report angular photoemission studies made on the (110) and (111) faces of W crystals for photon energies between 7.7 and 9.7 eV and analyze the data to obtain the location in wave-vector space of some of the direct transitions contributing to photoemission in this energy region.

As first discussed by Kane[4] in reference to angular photoemission measurements, only the tangential component of $\vec{k}$ is conserved when an electron of wave vector $\vec{k}$ propagates through the solid-vacuum interface. The normal component of $\vec{k}$ inside the crystal cannot be determined from a single measurement without detailed calculations of the internal band structure such as those performed by Mahan for simple metals.[5] We used Kane's idea to overcome this limitation by identifying the same transitions in angular photoemission data from the two different crystal surfaces. Peaks in emission from the two surfaces are identified with the same transition from the coincidence in energy and from considerations of smoothness and symmetry. The two components of $\vec{k}$ allow us to specify wave vectors for direct transitions occurring in the plane containing the ⟨111⟩ and ⟨110⟩ axes. For emission in other directions the reported measurements explicitly specify only two components of a three-component internal wave vector.

A more complete description of the experimental apparatus will be published in a later paper. Briefly, experiments were performed at pressures in the 10^{-10}-Torr range. The oriented single crystals were electropolished before pumpdown and cleaned by electron bombardment heating. Low-energy-electron diffraction was used to check sample surface condition and orientation.

The data reported here were taken with light incident at 60° from the sample normal. However, the direct transitions could be obtained with about the same intensity using normal photon incidence.

The forward hemisphere was covered by two angular motions. The detector was scanned in polar angle measured from the sample normal. Different azimuths were observed by rotating the sample about its normal. The angular resolution was about 3°. Magnetic fields in the electron-drift region were a few milligauss.

Energy analysis of photoemitted electrons was performed by a retarding-potential analyzer mounted in front of a particle-counting detector. Electron counts in an energy window of width ΔV centered on a retarding potential V_R were stored in the active channel of a multichannel scalar. By moving the detector as the multichannel scalar was stepped from channel to channel the polar angular distribution of photoemission was mapped at a given energy. Families of such curves taken at different azimuthal angles then provided complete information on the angular distribution of photoemission at a given retarding

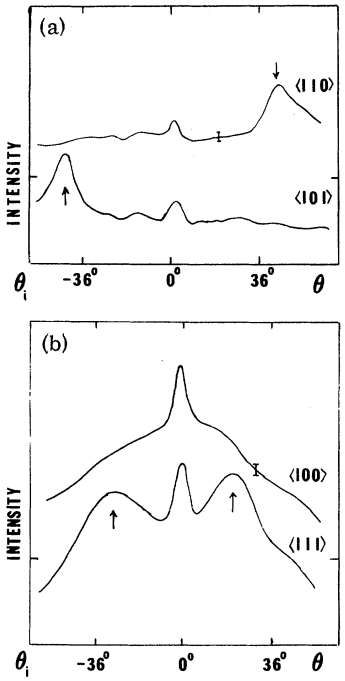

FIG. 1. Curves showing the spatial distribution of photoemission from (a) the (111) and (b) the (110) faces of W produced by 7.7 eV photons and with a −2.5-V retarding potential. Arrows indicate the prominent peaks produced by direct transitions. Principal symmetry directions through which the detector scanned are indicated.

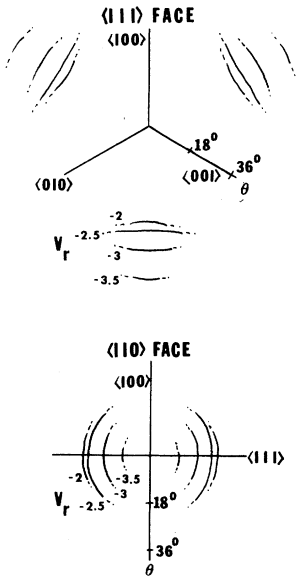

FIG. 2. Angular loci of strong direct transition peaks from W for a photon energy of 7.7 eV and a range of retarding voltages V_R. Two lobes of the pattern from the (111) face and most of the pattern from (110) face could be scanned during a single experiment. The polar angle θ is measured radially from the center of each plot.

voltage and photon energy. Figure 1 shows a few curves from two such families taken on the two single-crystal surfaces at a retarding potential of − 2.5 V for 7.7 eV photons. The scans were made in the symmetry planes defined by the sample-normal and off-normal symmetry directions that label the curves. The peak that appears close to the sample normal on all the curves is an artifact. The structures of interest for our analysis are the prominant peaks indicated by arrows that appear off the normal over restricted ranges of azimuthal angle. All angular structure showed threefold rotational symmetry on the (111) surface and twofold symmetry on the (110) surface as expected for the bcc crystal structure.

In Fig. 2 we plotted the angular positions of direct transition peaks for a photon energy of 7.7 eV and various retarding potentials in addition to $V_R = -2.5$ V. The peak positions for the curves were taken from families of curves like those shown in Fig. 1 made at different retarding potentials. The direct transitions give rise to emission cones centered on the ⟨110⟩ direction. Emission is strong in the plane defined by the ⟨111⟩ and ⟨110⟩ directions, but it is not confined to it. As one approaches the plane defined by the ⟨110⟩ and ⟨100⟩ directions emission from direct transitions disappears. Similar results are obtained at other photon energies up to about 9.7 eV, where this group of transitions disappears and is replaced by another group of transitions which gives rise to emission in the ⟨111⟩ direction.

The tangential component of the external electron momentum is

$$P_{\parallel} = (2mK)^{1/2} \sin\theta,$$

where K is the kinetic energy of the electrons in vacuum, m is the free-electron mass, and θ is the polar angle of emission. The tangential component of the crystal momentum k is then given by

$$\hbar k_{\parallel} = p_{\parallel}.$$

K is determined from the retarding potential and the position of the low-energy cutoff of the energy spectrum of photoemitted electrons.

After $k_{\parallel}$ for two different surfaces for the same transition have been determined from data like those shown in Figs. 1 and 2, the internal $\vec{k}$ may

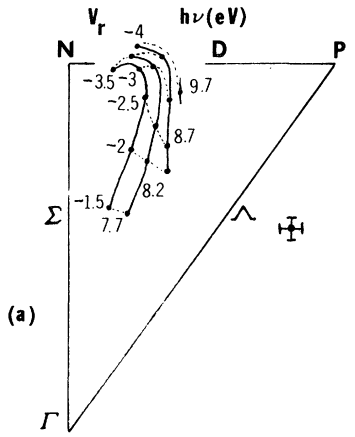

FIG. 3. Contours of constant band separation (——) and constant final state energy (----) in the ⟨111⟩-⟨100⟩ plane of $\vec{k}$ space for W.

be calculated for transitions in the ⟨110⟩-⟨111⟩ plane. If the positions of the transitions are calculated for a series of retarding potentials and a single photon energy the curve through these points gives the locus in the ⟨111⟩-⟨110⟩ planes of $\vec{k}$ space where the bands are separated an amount equal to the photon energy and there is an appreciable joint density of states for direct transitions. In Fig. 3 these joint-density-of-states curves are plotted as solid lines for photon energies between 7.7 and 9.7 eV. On this plot features of the Brillouin zone are indicated by the conventional symmetry notation. The data points along the arcs are labeled with the retarding voltage at which they were obtained. In Fig. 3 contours of constant final-state energy are drawn as dashed lines through the experimental points. These give a partial plot of levels of final-state energy ϵ_f measured from the Fermi level in the ⟨111⟩-⟨110⟩ plane of $\vec{k}$ space. Similar contour plots may be constructed through points of equal initial-state energy $\epsilon_i = \epsilon_f - h\nu$.

The results of Fig. 3 indicate that transitions are occurring between initial and final bands which increase in energy with increasing value of k. From the solid lines it is clear that the separation increases as one moves from the ⟨110⟩ toward the ⟨111⟩ direction. From the dashed lines, it is clear that the final-state energy also increases as the transitions approach the ⟨111⟩ direction. The opposite trend is found in the contours of initial energy. The sharp curvature near D probably reflects critical-point structure in the vicinity of the zone boundary.

Direct comparison of these results to published band-structure calculations is not possible since most of the transitions occur away from major symmetry directions. However, the trends noted in the previous paragraph may be compared to those expected from calculations for the Σ, Λ, and D symmetry directions.[6,7] In these calculations pairs of approximately parallel bands increase in energy from Γ along Λ and Σ to P and N, respectively. Both upper and lower bands are hybridized and split at large k. The separation of these bands is greater along the Λ than along the Σ direction, and the upper band is at higher energies along Λ than along Σ, in qualitative agreement with the trends we have observed.

The results reported also cannot be compared directly to the experimental work of other authors. The most relevant experimental study is that of Feurbacher and Fitton who studied emission normal to the (111), (110), and (100) faces of W. Above about 9.0-eV photon energy they observed electrons emitted normal to the (111) face which they attributed to direct transitions giving rise to emission in this direction. Our measurements in this energy region (not presented in this paper) confirm their results. In addition, at lower photon energies, they observed emission from both the (110) and (111) surfaces which they tentatively attributed to a surface emission process. We believe that these electrons are more probably produced by direct transitions and subsequently elastically scattered into the normal direction. This explanation assumes that this scattering is sufficiently isotropic to weaken the peaks due to direct transitions without altering their essential form or position. The electrons would then have the same energies as those produced by the strong direct transitions we have described in this paper. Also, no significant variation in the number of these normally emitted electrons was observed when the incident angle of the light was varied between 0° and 45°. A strong dependence would be expected for a surface emission process.

In this paper we have analyzed only a small part of the information available from the angular-emission experiments. The results presented lend credence to the assumption of tangential $\vec{k}$ conservation and to the applicability of direct transitions within a volume band structure for photoemission in W.

†Research supported by the National Science Foundation.

[1]B. Feurbacher and B. Fitton, Phys. Rev. Lett. 30, 923 (1973).

[2]N. V. Smith, M. M. Traum, and F. J. DiSalvo, Solid State Commun. 15, 211 (1974); also N. V. Smith and M. M. Traum, Phys. Rev. Lett. 31, 1247 (1973).

[3]U. Gerhardt and E. Dietz, Phys. Rev. Lett. 26, 1477 (1971); R. Y. Koyama and L. R. Hughey, Phys. Rev. Lett. 29, 1518 (1972); F. Wooten, T. Huen, and H. V. Windsor, Phys. Lett. 36A, 351 (1971); T. Gustafssons, P. O. Nilsson, and L. Walden, Phys. Lett. 37A, 121 (1971); and other references given in Ref. 2.

[4]E. O. Kane, Phys. Rev. Lett. 12, 97 (1964).

[5]G. D. Mahan, Phys. Rev. B 2, 4334 (1970).

[6]L. F. Mattheiss, Phys. Rev. 139, 1893 (1965); I. Petroff and C. R. Viswanathan, Phys. Rev. B 4, 799 (1971).

[7]N. E. Christensen, unpublished by author, band diagrams given in Ref. 1.

Low-Temperature Specific Heat of Polysulfur Nitride, $(SN)_x$

R. L. Greene, P. M. Grant, and G. B. Street
IBM Research Laboratory, San Jose, California 95193
(Received 25 September 1974)

Measurements of the specific heat of crystalline $(SN)_x$ in the region 1.5–10°K are reported. A linear temperature contribution to the specific heat is found and interpreted as arising from an electron state density of 0.18 state/(eV spin molecule) and a one-dimensional tight-binding conduction band of width ≥ 0.9 eV. Analysis of the lattice specific-heat contribution supports existing evidence that $(SN)_x$ is a highly anisotropic crystalline polymer and suggests a possible explanation for the apparent absence of a Peierls transition.

Much attention is currently being directed toward the study of conducting one-dimensional (1-D) systems.[1,2] Recently, Walatka, Labes, and Perlstein[3] (WLP) have suggested that the crystalline polymer polysulfur nitride, $(SN)_x$, may be another example of a 1-D conductor. They have reported metallic levels of dc electrical conductivity in $(SN)_x$ over the temperature range 4.2–300°K, in contrast to all other known 1-D conductors in which a metal-insulator transition occurs within this same temperature region. This exciting result clearly demonstrates that further studies on the properties of $(SN)_x$ are important for understanding the nature of 1-D conductors and should lend insight into ways to stabilize the metallic state in present and future 1-D materials. In pursuit of this objective, we report here the first specific-heat measurements on $(SN)_x$. These results, along with conductivity, thermopower, and magnetic-susceptibility data on our crystals, indicate that metallic behavior in $(SN)_x$ persists at temperatures down to 1.5°K. Our data enable an estimate of ~0.9 eV for the conduction-band width to be made on the basis of a simple 1-D tight-binding model. Moreover, the dependence of specific heat on temperature above 3.2°K gives clear evidence for the importance of anisotropic force constants in $(SN)_x$. An analysis of these data leads us to suggest that the Peierls transition may be suppressed by fluctuations in $(SN)_x$ because of weak interchain coupling.

Our samples were prepared in a manner similar to that described by WLP except that unpolymerized S_4N_4 and S_2N_2 were removed from the $(SN)_x$ by resublimation rather than by washing with benzene. The S_4N_4 starting material, carefully purified by recrystallization followed by gradient sublimation, was stored under vacuum before using. Chemical analysis of the resulting brass-colored $(SN)_x$ crystals indicated N, 29.60; S, 69.61 (calculated, N, 30.41; S, 69.59). The only other element found in a specific analysis was hydrogen [(0.2 ± 2)% by weight]. X-ray measurements on compressed samples agreed with the known x-ray structure[4] of $(SN)_x$ and gave no indication of S_4N_4 or S_2N_2 inclusions. Our x-ray data also gave no evidence of noncrystalline phases. Full details of the preparation and characterization of our $(SN)_x$ crystals will be presented elsewhere.

In order to compare our samples directly with those of WLP, we have performed conductivity and thermopower measurements between 1 and 300°K. The conductivity along the fibrous direction (each crystal being a bundle of parallel fibers) was measured by using a standard four-probe ac technique.[5] Typical room-temperature conductivities (σ_{RT}) averaged 600 $(\Omega\ \mathrm{cm})^{-1}$ with considerable variation among samples, it being difficult to accurately determine the cross-sec-